

# RESEARCH TO SIMULATE THE SHIP'S VIBRATION REGENERATION SYSTEM USING A 6-DEGREE FREEDOM GOUGH-STEWART PARALLEL ROBOT

Submitted: 7<sup>th</sup> November 2023; accepted: 19<sup>th</sup> December 2023

Nguyen Duc Anh, Nguyen Quang Vinh

DOI: 10.14313/JAMRIS/2-2024/10

## Abstract:

*This article presents research results on building a model to reproduce ship vibrations based on a parallel robot with 6 degrees of freedom on the Gough-Stewart platform. Vibration data at the ship's center of gravity, calculated by simulation software, will be inputted into the model. The regenerative control system uses a simple PID controller to control input trajectory tracking. Simulation results on Matlab/Simulink software have demonstrated the reproduction of ship vibrations within the allowable error.*

**Keywords:** robot, ship vibration reconstruction, vibration simulation

## 1. Introduction

The vibration of ships under the impact of ocean waves is one of the most complex types of oscillations. The study of ship vibrations plays an important role in ship design, installation, stable control of shipboard systems ship driving simulation [5, 11, 12]. Because the ship's vibration is complex, making actual measurements costs both money and time, it is difficult to cover all types of ships and different types of wave levels. Therefore, the study of reproducing ship vibrations on simulation models or semi-natural models is of great significance in steering simulation problems, especially in research problems of stable control systems equipment placed on board. The Gough-Stewart 6-degree-of-freedom parallel robot consists of a working stage (moving base) linked to a fixed base through six legs by ball or propeller joints. The robot has 6 legs that are driven by electric motors or hydraulic cylinders. The robot's structure allows movement in 6 degrees of freedom for the work stage by changing the length of each leg. Parallel robots can create vibrations similar to the actual vibrations of moving vehicles such as ships, cars, and airplanes. Therefore, parallel robots with 6 degrees of freedom of the Gough-Stewart platform are often used in flight simulation systems and ship-driving simulation systems [11]. In current practice, the problems of calculating and reproducing ship vibrations are mainly calculated based on 2D [13], or 3D models [5, 11]. They are mostly used in construction projects to simulate the motion of ships and serve the training process of ship drivers [11].

The oscillations reproduced in driving simulation systems are usually oscillations given in the form of harmonic functions. Simulation software allows use to change the amplitude and period of oscillations. Because the oscillations of ocean waves are very complex, modeling in the form of harmonic oscillations is not appropriate, they should be modeled based on the energy spectrum and direction of wave propagation. From the wave vibration data in digital form, the ship's vibration data in digital form can also be calculated as input to regenerate the ship's vibration. This is the main content that this article presents with the application of the 6-degree-of-freedom Gough-Stewart parallel robot model to reproduce vibrations. The next parts of the article include ocean wave models and ship motion models. Then the construction of a ship vibration reconstruction system, the content of simulation research, and the evaluation of results are provided.

### 1.1. Vibration of a Ship on Sea Waves

Ocean waves are formed by the impact of wind, astronomical gravity, and floating vehicles such as ships. They are often described by wave height, length, and period [2]. The vertical difference between the elevation of the adjacent crest and trough determines wave height. In This article introduces ocean waves formed due to the presence of wind. Ocean waves can be understood as a superposition of multiple harmonic waves, each of which has its amplitude, frequency, and phase, as can be seen in Figure 1 [4]. There are two main models to describe ocean waves [2]: one-dimensional waves (long-crested sea) in Figure 2 and multi-dimensional waves (Short-crested sea) in Figure 3. According to wind speed, ocean waves are divided into 10 levels from 0 to 9, corresponding to the wave's oscillation amplitude [2]. Many mathematical models describe the oscillations of different ocean waves such as wave models based on wave theories, wave models based on energy spectrum, and wave propagation direction. The vibration equations of ocean waves are based on wave theories such as Airy linear wave theory, Stokes wave theory, and Cnoidal wave theory presented in the documents model [3,10]. One accurate wave model is based on the energy spectrum and direction of wave propagation.

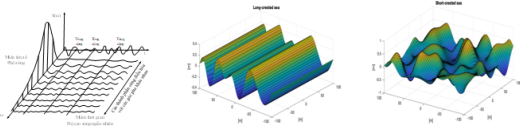


**Figure 1.** Superposition of waves and wave spectrum

Common types of wave energy spectra include the Neumann energy spectrum, Bretschneider energy spectrum, Pierson-Moskowitz energy spectrum, JON-SWAP energy spectrum, and Torsethaugen energy spectrum. In the framework of this article, a one-dimensional wave oscillation model is used to study ship oscillation and reproduce that oscillation. The ocean wave model equation, [8] is presented in equation (1) below:

$$\xi(x, y, t) = \sum_{i=1}^N \sqrt{S(\omega_i) \Delta \omega} \cos(k_i(x_i \cos(\mu) + y_i \sin(\mu) - \omega_i t + \varepsilon_i)) \quad (1)$$

where:  $k_i$ -wave number;  $\lambda_i$ -wave length of the  $i^{th}$  wave component;  $\omega$ -oscillation frequency;  $\varepsilon_i$ -Random phase of the  $i^{th}$  wave component;  $\Delta \omega$ -constant deviation between wave frequencies;  $\mu$ -wave direction angle;  $S(\omega)$ -energy spectrum of the wave. In this article, the Bretschneider energy spectrum is used with the following formula [2]:

$$S(\omega) = \frac{1.25}{4} \frac{\omega_0^4}{\omega^{-5}} H_s^2 \exp[-1.25(\omega_0/\omega)^4] \quad (2)$$

where:  $H_s$ : is the average wave height (the average of one-third of the height of the highest waves).

## 1.2. Ship Motion Model

Consider a ship with mass  $m$ , with dimensions of length, width and height denoted  $L$ ,  $B$ ,  $H$  respectively. The fixed  $G_0$  ( $OXYZ$ ) coordinate system is attached to the earth. Coordinate system  $G_1$  ( $ONVW$ ) is attached to the ship; the coordinate origin is at the center of gravity; the  $OX$  axis is along the ship's hull and points towards the bow of the ship; and the  $OZ$  axis is perpendicular to the ship's deck surface (Figure 2). State variables when studying ship motion include:  $[x, y, z, v_u, v_v, v_w, \phi, \theta, \psi, u, v, w]^T$  where:  $[x, y, z]^T$ - The position of the ship's center of gravity is described in a coordinate system attached to the earth;  $[v_u, v_v, v_w]^T$ -The velocity of the ship's center of gravity is described in a coordinate system attached to the ship;  $[\phi, \theta, \psi]^T$ -Euler angles describe the rotation of the coordinate system axes attached to the ship with the coordinate system axes attached to the earth;  $[u, v, w]^T$ -Rotational velocity in a fixed coordinate system attached to the ship. The relationship and identification of state variables are determined as follows:

$$\begin{bmatrix} \dot{x} & \dot{y} & \dot{z} \end{bmatrix}^T = \mathbf{R} \begin{bmatrix} v_u & v_v & v_w \end{bmatrix}^T \quad (3)$$

where  $\mathbf{R}$  is the number of rotations, determined according to the expression below:

$$\mathbf{R} = [\mathbf{A}]_{3 \times 3} \quad (4)$$

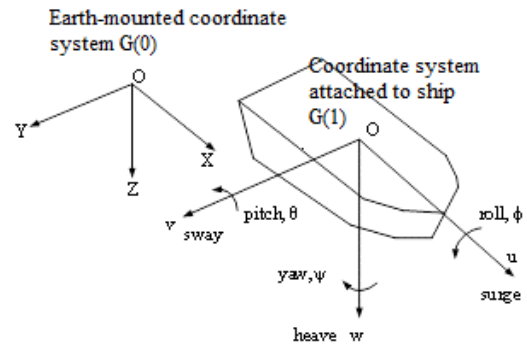


**Figure 2.** Ship models and coordinate systems

where:  $A_{11} = C(\psi)C(\theta)$ ;  
 $A_{12} = C(\psi)S(\theta)S(\phi) - C(\phi)S(\psi)$ ;  
 $A_{13} = S(\psi)S(\phi) + C(\phi)C(\psi)S(\theta)$ ;  $A_{21} = C(\theta)S(\psi)$ ;  
 $A_{22} = C(\psi)C(\phi) + S(\psi)S(\theta)S(\phi)$ ;  
 $A_{23} = C(\phi)S(\psi)S(\theta) - C(\psi)S(\phi)$ ;  $A_{31} = -S(\theta)$ ;  
 $A_{32} = C(\theta)S(\phi)$ ;  $A_{33} = C(\theta)C(\phi)$ ;  $C \triangleq \cos$ ;  
 $S \triangleq \sin$  The velocity of the ship's center of gravity is determined as follows [2]:

$$\begin{bmatrix} \dot{v}_u \\ \dot{v}_v \\ \dot{v}_w \end{bmatrix} = \begin{bmatrix} -\frac{C_{d,u} A_u \rho}{m} v_u + \frac{1}{m} F_u \\ -\frac{C_{d,v} A_v \rho}{m} v_v + \frac{1}{m} F_v \\ -\frac{C_{d,w} A_w \rho}{m} v_w + \frac{1}{m} F_w \end{bmatrix} - \begin{bmatrix} u \\ v \\ w \end{bmatrix} \times \begin{bmatrix} v_u \\ v_v \\ v_w \end{bmatrix} \quad (5)$$

where:  $C_d$ :damping constant of velocity;  $\rho$ -density of water;  $m$ : mass of the ship;

$$\begin{bmatrix} \dot{\phi} & \dot{\theta} & \dot{\psi} \end{bmatrix}^T = \mathbf{T} \begin{bmatrix} u & v & w \end{bmatrix}^T \quad (6)$$

The transfer matrix  $\mathbf{T}$  is defined as follows:

$$\mathbf{T} = \begin{bmatrix} 1 & \sin(\phi) \tan(\theta) & \cos(\phi) \tan(\theta) \\ 0 & \cos(\phi) & -\sin(\phi) \\ 0 & \cos(\phi) \sec(\theta) & \cos(\phi) \sec(\theta) \end{bmatrix} \quad (7)$$

The rotational acceleration in a fixed coordinate system attached to the ship is determined as follows [2]:

$$\begin{bmatrix} \dot{u} \\ \dot{v} \\ \dot{w} \end{bmatrix} = \begin{bmatrix} -\frac{B_u}{I_u} u + \frac{1}{I_u} \tau_u \\ -\frac{B_v}{I_v} v + \frac{1}{I_v} \tau_v \\ -\frac{B_w}{I_w} w + \frac{1}{I_w} \tau_w \end{bmatrix} \quad (8)$$

where:  $B_u, B_v, B_w$ -Torsional memory friction coefficient  $[N.s/m]$ ;  $I_u, I_v, I_w$ -Moment of inertia of the ship according to the pillars  $Ou, Ov, Ow$  of the coordinate system attached to the ship;  $\tau_u, \tau_v, \tau_w$  - Total external force moment acting on the ship's hull. In this article, for simplicity we assume the ship is in the anchored position, the propeller does not move, ignoring the mass added to the ship, the force of the wind, and the forces acting on the ship include the thrust of the water (force hydrostatic force), gravity, Coriolis force and centripetal inertial force. Therefore, the train's equation of motion in [2] can be written in a simple form as follows:

$$\mathbf{M}_{RB} \dot{\mathbf{v}} + (\mathbf{C}_{RB} + \mathbf{D}_v) \mathbf{v} = \boldsymbol{\tau} \quad (9)$$

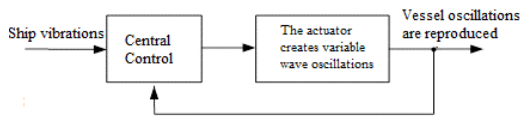


**Figure 3.** Block diagram of ship vibration regeneration system

where:  $\mathbf{v} = [\dot{x} \ \dot{y} \ \dot{z} \ \dot{\phi} \ \dot{\theta} \ \dot{\psi}]^T$  - velocity vector of coordinate system G1 relative to coordinate system G0;  $\mathbf{M}_{RB}$  - mass matrix and inertia tensor of the ship;  $\mathbf{I}_{G1}$  is the ship's inertial tensor with respect to the G1 coordinate system;  $\mathbf{D}_v$  - linear viscous friction damping matrix;  $\mathbf{C}_{RB}$  - matrix with components due to the Coriolis inertia force [14] and the ship's radial inertia force. The wave model and ship motion model presented in this section have been used in the wave simulation and ship simulation toolkit of the LINK-SIC center at Linköping University [7]. The simulation process and results using this tool are presented in section 4 of this article.

## 2. Building a Ship Vibration Reconstruction System

### 2.1. Block Diagram of Ship Vibration Reconstruction System

Figure shows the block diagram of the ship vibration signal reconstruction system. This system includes two main components: the ship's oscillating actuator and the controller. The ship vibration regeneration system has the following working principle: When the system's input has ship vibration signals, the system's controller will rely on the input signal and feedback signal to create the signals. The actuator control signal oscillates according to the input signals. In this paper, we use ship vibration signals from the simulation toolkit of the LINK-SIC center with the input information being position and Euler angles; The actuator uses a 6-degree-of-freedom parallel robot model (the Gough–Stewart platform) [1]; The controller uses a PID controller. Solving kinematic problems of parallel robots and calculating and designing controllers are presented in detail below.

### 2.2. Parallel Robot Inverse Kinematics Model

The robot's kinematic diagram is shown in Figure 4. The fixed base and working stages of the robot are respectively denoted  $B_1, P_1$  the center of joints on base  $B_1$  and center of joints on link  $P_1$  are denoted as  $B_{1i}, P_{1i}$  respectively ( $i = 1..6$ ). The fixed coordinate system  $O_0X_0Y_0Z_0$  is mounted at the center of the base  $B_1$ , the  $O_0Z_0$  axis points up, the  $X_0$  axis passes through the midpoint of the line connecting the two joints  $B_{11}$  and  $B_{16}$ . The coordinate system  $O_1X_1Y_1Z_1$  is attached to the center at point  $P_1$ , with the  $O_1Z_1$  axis pointing up, and the  $O_1X_1$  axis passing through the midpoint of the line connecting  $P_{11}$  and  $P_{16}$ . The Stewart-Gough type parallel robot has joints located on a fixed base or working link B1 arranged in symmetrical pairs and located on the same circle.

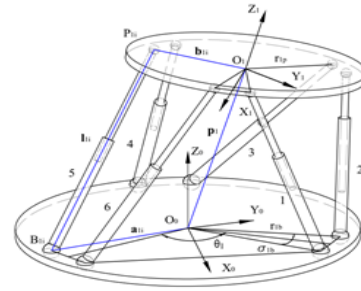


**Figure 4.** Parallel robot kinematic diagram

The angle between  $O_0B_{11}$  and  $O_0B_{13}$  is  $120^\circ$ , the angle between  $O_0P_{11}$  and  $O_0P_{13}$  is  $120^\circ$ . Let the radius of the circle created by the joints on surface B1 and the radius of the circle created by the joints on surface P1 be  $r_{1b}$  and  $r_{1p}$  respectively. The angle  $B_{11}O_0B_{12}$  is  $\sigma_{1b}$ . The angle  $P_{11}O_0P_{12}$  is  $\sigma_{1p}$ . The angle between axis  $O_0X_0$  and vector  $a_{1i}$  is  $\xi_{1i}$ , the angle between axis  $O_1X_1$  and vector  $b_{1i}$  is  $\zeta_{1i}$ . The distances from the center of the base B1 and the joint P1 to their respective joint centers are  $a_{1i}$  and  $b_{1i}$  respectively. The lengths of the legs are  $l_{1i}$ ,  $i = 1, \dots, 6$  respectively.

$$\begin{aligned} \xi_{1i} &= \frac{\theta_{1i}}{2} - \frac{\sigma_{1b}}{2}; \quad \zeta_{1i} = \frac{\theta_{1i}}{2} - \frac{\sigma_{1p}}{2}; \quad i = 1, 3, 5 \\ \xi_{1i} &= \xi_{1i-1} + \sigma_{1b}; \quad \zeta_{1i} = \zeta_{1i-1} + \sigma_{1p}; \quad i = 2, 4, 6 \end{aligned} \quad (10)$$

The center position of the joints in the corresponding coordinate systems attached to the base and working link is determined as follows:

$$\begin{aligned} {}^0\mathbf{a}_{1i} &= \begin{bmatrix} r_{1b} \cos(\xi_{1i}) & r_{1b} \sin(\xi_{1i}) & 0 \end{bmatrix}^T \\ {}^1\mathbf{b}_{1i} &= \begin{bmatrix} r_{1p} \cos(\zeta_{1i}) & r_{1p} \sin(\zeta_{1i}) & 0 \end{bmatrix}^T \end{aligned} \quad (11)$$

The generalized coordinates of the robot in joint space include the length variables of the 6 legs:

$$\mathbf{q}_1 = [l_{11} \ l_{12} \ l_{13} \ l_{14} \ l_{15} \ l_{16}]^T = [\mathbf{l}_{1i}]^T \quad (12)$$

The vector determines the position and direction of the working stage:

$$\mathbf{p}_1 = [x_1 \ y_1 \ z_1 \ \alpha_1 \ \beta_1 \ \gamma_1]^T \quad (13)$$

The rotation matrix from the  $O_1$  coordinate system to the  $O_0$  coordinate system corresponding to the roll, pitch, yaw angles  $\gamma, \beta, \alpha$  is:

$$\mathbf{R}_{01} = C_{3 \times 3} \quad (14)$$

where:  $C_{11} = C(\gamma_1)C(\beta_1)$ ;  $C_{21} = C(\beta_1)S(\gamma_1)$ ;  $C_{31} = -S(\beta_1)$ ;  $C_{12} = C(\gamma_1)S(\beta_1)S(\alpha_1) - C(\alpha_1)S(\gamma_1)$ ;  $C_{22} = C(\gamma_1)C(\alpha_1) + S(\gamma_1)S(\beta_1)S(\alpha_1)$ ;  $C_{32} = C(\beta_1)S(\alpha_1)$ ;  $C_{13} = S(\gamma_1)S(\alpha_1) + C(\alpha_1)C(\gamma_1)S(\beta_1)$ ;  $C_{23} = C(\alpha_1)S(\gamma_1)S(\beta_1) - C(\gamma_1)S(\alpha_1)$ ;

$C_{33} = C(\beta_1)C(\alpha_1)$ ;  $C \triangleq \cos$ ;  $S \triangleq \sin$

The length vector of a robot leg is calculated as follows:

$$\vec{l}_{1i} = \vec{p}_1 + \vec{b}_{1i} - \vec{a}_{1i} \quad (15)$$

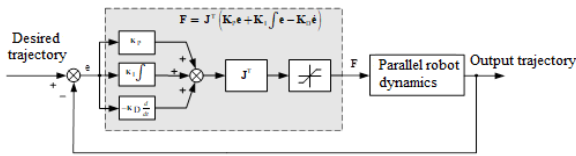


**Figure 5.** Control diagram of the ship vibration regeneration system

Project the vector equations to the  $O_0$  coordinate system:

$${}^0\mathbf{l}_{1i} = {}^0\mathbf{p}_1 - {}^0\mathbf{a}_{1i} + {}^0\mathbf{b}_{1i} = {}^0\mathbf{p}_1 - {}^0\mathbf{a}_{1i} + \mathbf{R}_{01} {}^1\mathbf{b}_{1i} \quad (16)$$

$${}^0\mathbf{l}_{1i} = \begin{bmatrix} m_{11} & m_{12} & m_{13} \\ m_{21} & m_{22} & m_{23} \\ m_{31} & m_{32} & m_{33} \end{bmatrix} \begin{bmatrix} p_{1ix} \\ p_{1iy} \\ p_{1iz} \end{bmatrix} + \begin{bmatrix} x_1 - b_{1ix} \\ y_1 - b_{1iy} \\ z_1 - b_{1iz} \end{bmatrix}$$

$$= \begin{bmatrix} m_{11}p_{1ix} + m_{12}p_{1iy} \\ m_{21}p_{1ix} + m_{22}p_{1iy} \\ m_{31}p_{1ix} + m_{32}p_{1iy} \end{bmatrix} + \begin{bmatrix} x_1 - b_{1ix} \\ y_1 - b_{1iy} \\ z_1 - b_{1iz} \end{bmatrix} \quad (17)$$

Note above that  $p_{1iz}$  is 0. The length of one leg of the robot is calculated as follows:

$$l_{1i}^2 = x_1^2 + y_1^2 + z_1^2 + 2(m_{11}b_{1ix} + m_{12}b_{1iy})(x_1 - a_{1ix}) + r_{1p}^2 + r_{1b}^2 + 2(m_{21}b_{1ix} + m_{22}b_{1iy})(x_1 - a_{1iy}) + 2(m_{31}b_{1ix} + m_{32}b_{1iy})z_1 - 2(x_1a_{1ix} + y_1a_{1iy}) \quad (18)$$

Based on equations (17), (18), the leg lengths will be calculated according to the variables in the working space.

### 3. Controller Design

The basic goal of the controller for the ship vibration regeneration system is that based on the desired trajectory of the working stage  $P_1$  including position and direction, it will be calculated into the corresponding desired trajectory at the leg using inverse kinematics. Finally, a controller for each leg is used to control the legs to follow that desired trajectory. In this way, we get the fluctuations of the working stage following the fluctuations.

$$\mathbf{M}(\mathbf{X})\ddot{\mathbf{X}} + \mathbf{h}(\mathbf{X}, \dot{\mathbf{X}}) = \mathbf{J}^T \mathbf{F} \quad (19)$$

Using the parallel robot dynamics model in [6] and expressed in expression (19). In which:  $\mathbf{M}(\mathbf{X})$  is the inertia matrix;  $\mathbf{h}(\mathbf{X}, \dot{\mathbf{X}})$  is a matrix consisting of nonlinear components including Coriolis force [9, 10], centripetal force and gravity force;  $\mathbf{F} = \{F_1, F_2, \dots, F_6\}^T$  force vectors of corresponding legs;  $\mathbf{J}$  is the Jacobian matrix. To keep it simple, in this paper, we design a simple PID controller with the input being the position error and the error velocity, and the output being the force vector on the pins. The control diagram of the system is presented in Figure 5 This section will present simulation content, including ocean wave and ship vibration simulations.

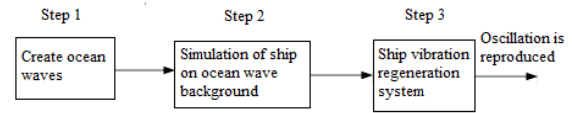


**Figure 6.** Sequence of simulation step

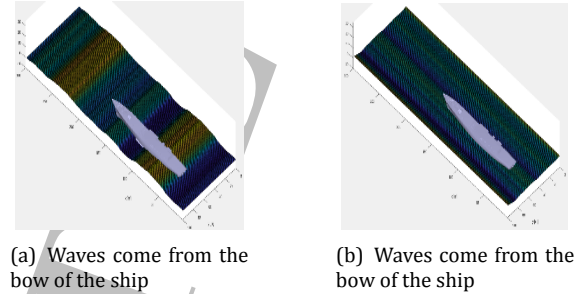


**Figure 7.** Simulation results of level 6 waves and ships on waves in 02 directions

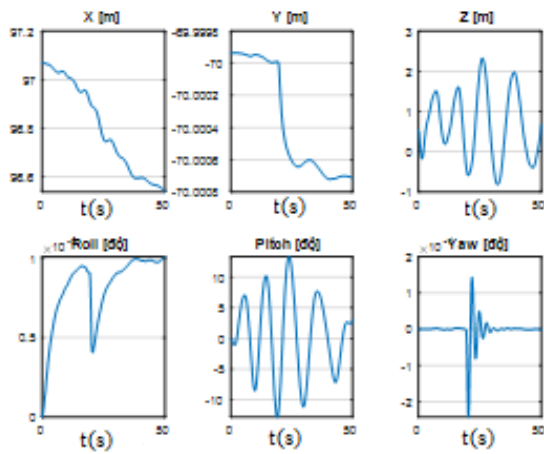
Signals simulating ship vibrations will be input into the vibration reconstruction system. The sequence of steps will be illustrated in Figure 6 below.

#### 3.1. Simulate Ocean Waves

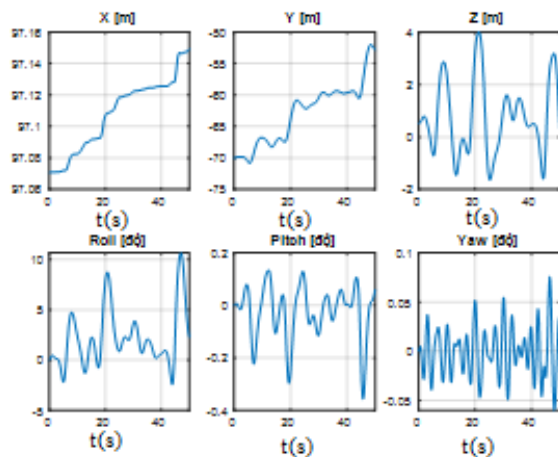
In this ocean wave simulation, in order not to lose generality as well as simulation volume, this article conducts 02 simulations of level 6 waves of one-dimensional wave type with wave model (1) and spectrum (2) according to 2 directions relative to the ship: waves entering the ship's bow  $180^\circ$  and waves perpendicular to the ship's side  $90^\circ$ . Wave simulation software of LINK-SIC center [7]. The wave simulation results are presented in Figure 7.

#### 3.2. Simulating Ship Vibrations

After receiving the wave simulation results, the ship's vibrations are simulated. The ship parameters used are as follows: Vessel length ( $L$ )=137m; Amount of water occupied ( $D$ ) =  $25 \cdot 10^5 \text{N}$ ; Ship width ( $B$ )=15m; Ship height ( $H$ )=16m; Height of ship's center of gravity ( $Z_g$ ) = 2,5m. Using the ship simulation program of LINK-SIC [7] with the simulation condition that the ship is anchored, the simulation results in Figure 8 are the oscillations of the ship's center of gravity corresponding to the wave directions. From the ship vibration simulation results in Figure 8, we can see the following points: 1) The X and Y parameters of the ship's center of gravity change small and follow a linear form, true to react when there is impact wave; 2) Z-parameter fluctuations are significant with amplitudes up to 4m (wave level 6 has wave amplitudes up to 6m); 3) Euler angles react with amplitudes less than 10 degrees. From these comments, when applied to the ship vibration reconstruction system, we need to process this signal because the Z-axis travel parameters of the parallel robot are difficult to guarantee up to 6m and the parameters in terms of X and Y coordinates can be equal to zero.



(a) Waves come from the bow of the ship



(b) Waves come from the bow of the ship

**Figure 8.** Simulation results of ship vibrations on level 6 waves coming from the ship’s bow

Therefore, the input to the ship oscillator system focuses on parameters along the Z-axis and Euler angles.

**3.3. Simulate the Oscillation Regeneration System**

The Gough-Stewart 6-degree-of-freedom parallel robot model in this article uses the parameters of the eMotion-1500/2700-6DOF-650-MK1 parallel robot from Bosch Rexroth. The basic parameters of the eMotion-1500 parallel robot are as follows: Fixed base ( $r_i (m)=1,28$ ;  $h_i (m)= 0,172$ ;  $\theta_i =120$ ;  $\sigma_i=8,6$ ); Work stage ( $r_i (m)=0,931$ ;  $h_i (m)= 0,152$ ;  $\theta_i =120$ ;  $\sigma_i=20,6$ ); The mass of the robot moving part does not include the load: 1755 kg; Maximum load: 1500 kg; Weight of 1 foot:140 kg; Journey of one leg:0,62m or Height of working plane at lowest position:1,25m.

Matlab Multibody tool [13]. The input to the model is the fluctuation at the ship’s center of gravity position. These oscillations have been processed to match the movements of the eMotion-1500 robot. This input signal has been processed with ref index in Figures 13 to 16 below. PID controller parameters for oscillation regeneration system  $K_p = 5.10^4$ ,  $K_i = 2.10^4$ ,  $K_D = 4.10^3$ .

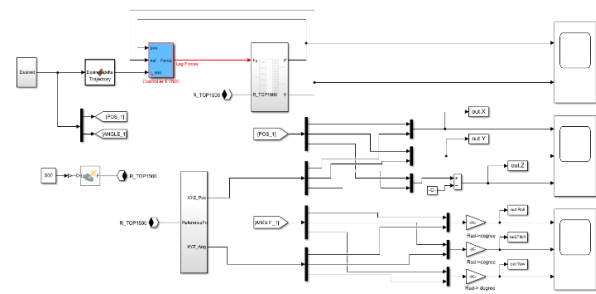
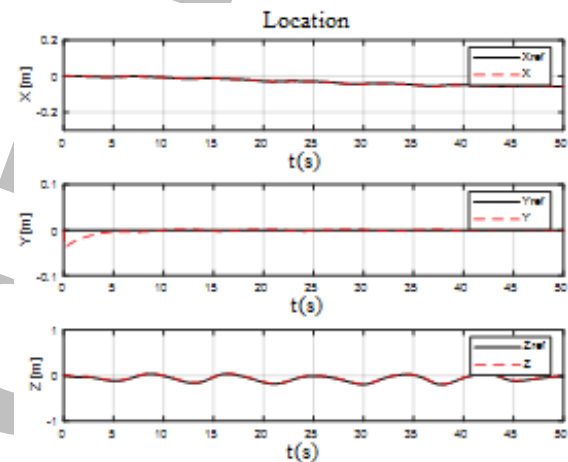
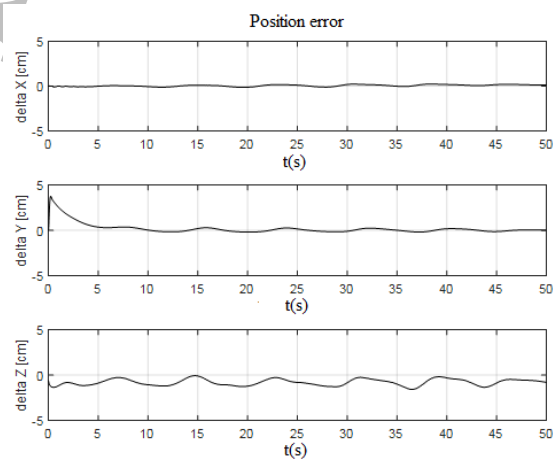


**Figure 9.** Simulation diagram of the vibration regeneration system on Matlab/Simulink



(a)



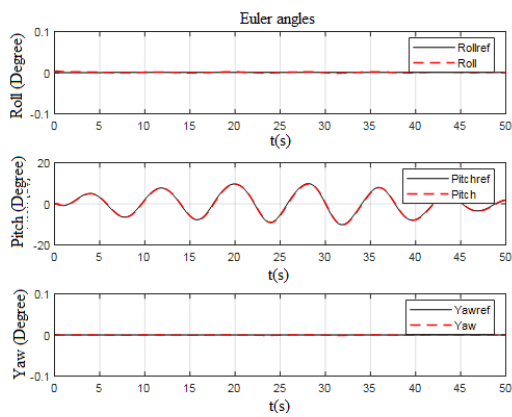
(b)

**Figure 10.** Graph reproducing the fluctuation center position and the error of the ship’s when the wave go straight in the ship’s bow

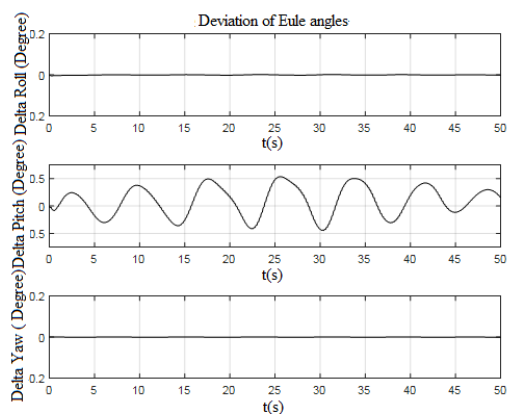
The simulation model of the ship’s vibration regeneration system using the eMotion-1500 parallel robot with PID controller on Matlab software is presented in Figure 9.

From the simulation model in Figure 9, the oscillation regeneration system is simulated with the following cases:

**Case 1:** Vibration of the ship with a level 6 unidirectional wave coming from the ship’s bow Figure 7 a.



(a)



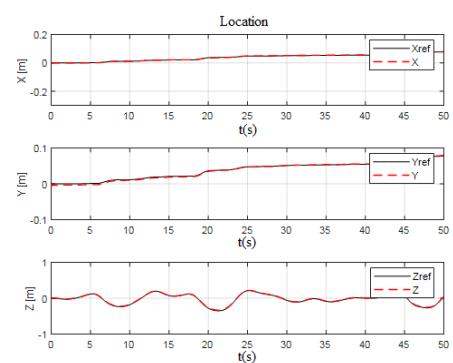
(b)

**Figure 11.** Graph reproducing fluctuations Euler angles and errors of ship when waves go straight in the ship’s bow

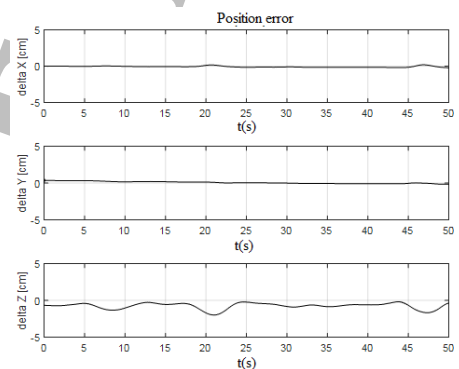
The input signal of the Ship Vibration Regeneration System in Figure 7 a has been processed into X and Y channel signals into small oscillations, while the Z channel is regulated for the maximum motion capability of the eMotion-1500 parallel wave robot working stage. Simulation results of position, Euler angle and corresponding error of this case are presented in Figure 10 and Figure 11.

**Case 2:** Vibration of the ship with level 6 unidirectional waves coming from the side of the ship (Figure 7 b). The input signal of the Ship Vibration Regeneration System in Figure 7 b) is similarly processed as the X and Y channel signals into small oscillations, while the Z channel is regulated for the maximum movement ability of the robot work stage eMotion-1500 wave. The simulation results of this case are presented in Figure 12 and Figure 13.

**Evaluation:** From the above two simulation cases, it can be observed that the ship vibration regeneration system designed above has created vibrations that follow the input vibrations with small errors in both position and direction. The error is small for position, the error is less than 5 cm, while the error is less than 1 degree for waves with the largest wave height of 4-6 m, with a period of about 20-25. This is a large wave level and is often the critical threshold for control and stabilization systems installed on ships.

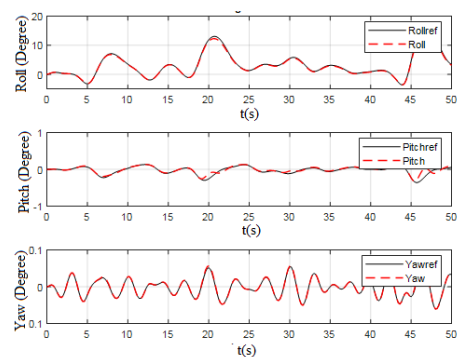


(a)

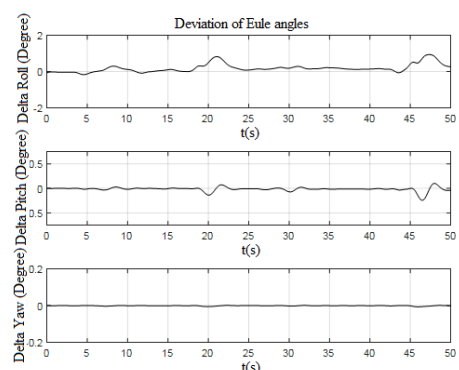


(b)

**Figure 12.** Graph reproducing center position fluctuation and error the ship’s when waves go straight in the ship’s side



(a)



(b)

**Figure 13.** Graph reproducing the fluctuations of the ship’s center Euler angles and the errors when waves enter the ship’s bow

#### 4. Conclusion

The article has presented research on a one-dimensional (long-crested) ocean wave model, a model of ship motion and its oscillations on a given wave background with two cases of waves traveling from the ship's bow (180 degrees) and waves hitting the side of the ship (90 degrees) when the ship stands at anchor, these studies used the LINK-SIC program suite. The study of wave and vibration models plays an important role in building a simulation model of the Vibration Regeneration System with a 6-degree-of-freedom Gough-Stewart parallel robot. The vibration reconstruction system model of the ship's center of gravity is obtained on Matlab/Simulink software through the Matlab Multibody tool which processes the input signal to suit the system and simulate the system. The simulation results ensure the accuracy of reproducing ship vibrations. From these results, the article has solved the problem of reproducing ship centerline oscillations as a basis for creating oscillations at any position of the ship, serving research on other problems (e.g. installing weapon stabilization systems, electro-optical sights, etc.). The results of this research serve as a basis for performing vibration reconstruction on a real robot system in step 1, step 2 (Figure 6) will be performed by actual measurements, while step 3 will be demonstrated on a realistic 6-degree-of-freedom Gough-Stewart parallel robot system.

#### AUTHORS

**Nguyen Duc Anh** – University of Fire Prevention and Fighting, 174 Khat Duy Tien, Ha Noi, Viet Nam, e-mail: anhpcph@gmail.com, www: daihocpccc.edu.vn.

**Nguyen Quang Vinh\*** – Academy of Military Science and Technology, Hoang Sam, Ha Noi, Viet Nam, e-mail: vinhquang2808@gmail.com, www: vinhquang2808.wordpress.com.

\*Corresponding author

#### References

- [1] Nguyen, C., Antrazi, S., Zhou, Z. and Campbell Jr, C. Analysis and implementation of a 6 DOF Stewart Platform-based robotic wrist. *Computers and Electrical Engineering*. 17, 191–203 (1991). doi: 10.1016/0045-7906(91)90035-X.
- [2] Fossen, T. Handbook of marine craft hydrodynamics and motion control. (John Wiley and Sons, 2011).
- [3] Vinh, N. and Van Phuc, P. Control of the Motion Orientation of Autonomous Underwater Vehicle. *Procedia Computer Science*. 150 pp. 69-77 (2019). doi: 10.1016/j.procs.2019.02.015.
- [4] Faltinsen, O. Sea loads on ships and offshore structures. (Cambridge university press,1993). ISBN-10: 0521458706.
- [5] Ghadimi, P., Dashtimanesh, A., Faghfoor Maghrebi, Y. and Others Initiating a mathematical model for prediction of 6-DOF motion of planing crafts in regular waves. *International Journal Of Engineering Mathematics*. 2013 pp. 1–16 (2013). doi: 10.1155/2013/853793.
- [6] Taghirad, H. Parallel robots: Mechanics and control. (CRC press,2017. ISBN-10: 1138077380, ISBN-13: 978-1138077386.
- [7] Wu, H., Wu, Y., Zhang, Y. and Zhang, Y. Intelligent encryption method for wireless sensing signal of underwater vehicles. *International Journal Of Vehicle Information And Communication Systems*. 7, 366–380 (2022). doi: 10.1504/IJVICS.2022.129034.
- [8] Debnath, L. Nonlinear water waves. Academic Press: San Diego. (1994). ISBN 0-12-208437-3. xviii, 544 pp.
- [9] Vinh, N., Duc Thanh, N., Minh Dac, H. and Dang Khoa, T. Identify aerodynamic derivatives of the airplane attitude channel using a spiking neural network. *International Journal Of Aviation, Aeronautics, And Aerospace*. 7, 3 (2020). doi: 10.15394/ijaaa.2020.1490.
- [10] Kornev, N. Ship dynamics in waves. (University Rostock, Germany 2012)
- [11] Shenhua, Y., Xinghua, W. and Guoquan, C. Design and implement on intelligent ship handling simulator. *2010 International Conference On Digital Manufacturing and Automation*. 1 pp. 473–477 (2010). doi: 10.1109/ICDMA.2010.216.
- [12] Xiufeng, Z., Yicheng, J., Yong, Y., Hongxiang, R. and Xiuwen, L. Ship motion modeling and simulation in Ship Handling Simulator. *2012 International Conference On Audio, Language And Image Processing*. pp. 1051–1056 (2012). doi: 10.1109/ICALIP.2012.6376771.
- [13] Yan, J., Jia, F., Qian, C. & Fang, Y. A MATLAB Multi-Body Simulation Platform Toward Multiple Flapping Wing Vehicles. *2023 42nd Chinese Control Conference (CCC)*. pp. 4574-4579 (2023). doi: 10.23919/CCC58697.2023.10239965.
- [14] Karapetkov, S., Uzunov, H., Dechkova, S. & Uzunov, V. Impact of inertial forces on car occupants in a vehicle-fixed barrier front crash. *Symmetry*. 15, 1998 (2023). doi: 10.3390/sym15111998.